Vrije Universiteit Brussel

Time-Variant Frequency Response Function Measurements on Weakly Nonlinear, Arbitrarily Time-Varying Systems Excited by Periodic Inputs

Pintelon, Rik; Louarroudi, Ebrahim; Lataire, John

Published in:
IEEE Transactions on Instrumentation and Measurement

DOI:
10.1109/TIM.2015.2426351

Publication date:
2015

Document Version:
Submitted manuscript

Link to publication

Citation for published version (APA):
Pintelon, R., Louarroudi, E., & Lataire, J. (2015). Time-Variant Frequency Response Function Measurements on Weakly Nonlinear, Arbitrarily Time-Varying Systems Excited by Periodic Inputs. *IEEE Transactions on Instrumentation and Measurement*, *64*(10), 2829-2837. https://doi.org/10.1109/TIM.2015.2426351

Copyright
No part of this publication may be reproduced or transmitted in any form, without the prior written permission of the author(s) or other rights holders to whom publication rights have been transferred, unless permitted by a license attached to the publication (a Creative Commons license or other), or unless exceptions to copyright law apply.

Take down policy
If you believe that this document infringes your copyright or other rights, please contact openaccess@vub.be, with details of the nature of the infringement. We will investigate the claim and if justified, we will take the appropriate steps.

Download date: 18. Apr. 2024

Time-Variant Frequency Response Function Measurements on Weakly Nonlinear, Arbitrarily Time-Varying Systems Excited by Periodic Inputs

R. Pintelon, E. Louarroudi, and J. Lataire
Vrije Universiteit Brussel, dept. ELEC, Pleinlaan 2, 1050 Brussel, Belgium
Tel. (+32-2) 629.29.44, Fax. (+32-2) 629.28.50, E-mail: Rik.Pintelon@vub.ac.be

***Abstract*—In quite some applications the linear dynamics of the system under test evolve over time in a smooth, non-periodic manner. The dynamic behavior of such systems is uniquely described by the time-variant frequency response function. However, since most real life systems behave to some extent nonlinearly, it is important to detect and quantify the deviation between the ideal linear time-variant framework and the true nonlinear time-variant dynamics. Therefore, in this paper a nonparametric estimation procedure is developed for detecting and quantifying the noise level and the level of the nonlinear distortions in time-variant frequency response function measurements using random phase multisine excitations. As a result, the users can decide whether or not the linear time-variant framework is accurate enough to describe the true dynamics in their particular application. The proposed measurement procedure is illustrated on a time-variant electronic circuit.**

***Index Terms*—time-variant frequency response function, time-variant systems, arbitrary time-variation, nonparametric estimates, nonparametric noise model, nonlinear distortions, periodic excitations, multisine**

I. Introduction

The true dynamics of a system under test do often not meet the classical linearity and time-invariance assumptions. This is the case in, for example, pit corrosion of metals where the time-variation is induced by the changes in the metal surface [1]; thermal drift in power electronics whose characteristics are temperature dependent [2]; aging, fatigue and mortification in biomedical measurements [3]; airplane dynamics which depend on the changing flight speed and height [4]; and battery impedance measurements which depend on the changing state-of-charge [5]. For all these applications the dynamics evolve smoothly and non-periodically over time in either an uncontrolled (pit corrosion; thermal drift; aging, fatigue and mortification) or a controlled (airplane dynamics, battery impedance measurements) way. The time-variant frequency response function (TV-FRF) introduced in [6], [7] uniquely characterizes the time-variant dynamics of these complex systems. However, since these real life systems all behave to some extent nonlinearly, there is a need to detect and quantify the deviation between the ideal linear time-variant framework inherent to the concept of the TV-FRF and the true nonlinear time-variant dynamics. No solution is available in the literature for non-periodic (arbitrary), smooth time-variations and the major goal of the present paper is to fill this important gap.

In some applications the time-variation originates from the switching between a finite number of linear time-invariant systems and, hence, is non-smooth. Examples of non-smooth time-variant dynamics can be found in power electronics [8], econometrics [9], and control applications [10]; and more general, in hybrid systems (see [11] and the references therein). In this paper we explicitly exclude non-smooth time-variations.

[12] presents an indirect method for measuring the TV-FRF of periodically time-varying systems excited by multisine excitations. Assuming that the periodic excitation can be synchronized with the periodic time variation, the noise level and the level of the nonlinear distortions are quantified (the algorithm described in [13] cannot detect and quantify the nonlinear distortions). The approach of [12] has been implemented in a small size, low cost frequency response analyzer [14]. [15] and [16] handle arbitrarily time-varying systems excited by, respectively, random phase multisine and arbitrary excitations. In both cases the nonlinear distortions can neither be detected nor quantified. Compared with the direct [15] and indirect [16] methods, the indirect procedure proposed in this paper has the following advantages:

- A few periods of the transient response to a random phase multisine excitation are sufficient (many periods are needed in [15]).
- Detection and quantification of the noise and the nonlinear distortions.
- The estimation procedure only requires nonparametric algorithms for multiple-input, single-output linear time-invariant systems ([15] requires dedicated algorithms for single-input, single-output time-variant systems).

Its major drawback is the fixed choice of the basis functions (Legendre polynomials) parametrizing the time-variation in the TV-FRF.

The nonparametric TV-FRF estimation methods based on the short-time Fourier transform assume that the time-variation is (very) slow (e.g. [17] for noise power spectra and [18] for FRFs). Hence, these methods inherently make a trade-off between accurate tracking of the time-variation (by minimizing the length of the sliding time window) and the required frequency resolution of the FRF measurement (by maximizing the length of the sliding time window). At the cost of a more complicated estimation algorithm, the approach proposed in this paper results in TV-FRF estimates with a much larger frequency resolution.

Since the time-variations considered are non-periodic (arbitrary), the estimated TV-FRF is valid in the measurement interval only. Without additional assumptions (e.g. ergodicity

of the time-variation) nothing can be said outside this interval. Nevertheless, the TV-FRF is still very useful for analyzing the time-variant dynamics. Indeed, the arbitrary (non-periodic) time-variation either can be controlled via (an) external scheduling parameter(s) (e.g. the flight speed and height in airplane dynamics) or is due to an uncontrollable physical phenomenon (e.g. the surface roughness in pit corrosion of metals). In the controlled case, the ultimate goal of the non-periodic time-variant experiments is to construct a linear differential equation whose coefficients depend on the external scheduling parameter(s) (= linear parameter-varying model). Analyzing the TV-FRF of these experiments is a first step to get insight into the complexity of this modeling problem (the dynamic order, and the (dynamic) dependency on the scheduling parameter(s)). In the uncontrolled case, it is difficult to the repeat the time-variant experiment under exactly the same conditions. Nevertheless, beside deep physical insight, the proposed TV-FRF estimation procedure allows one to distinguish the time-variant effects from the noise, the nonlinear distortions, and the experimental repeatability.

The outline of the paper is as follows. First, the class of nonlinear time-variant systems (Section II) and the class of excitation signals (Section III) for which the theory applies are described. Next, using the assumptions described in Section IV, and combining the results of [16], [19], [20] in an original and non-trivial way, an indirect method is developed for estimating nonparametrically the TV-FRF, its noise variance, and its variance due to the nonlinear distortions. Further, the proposed indirect method is illustrated on measurements of a time-variant electronic circuit (Section VI). Finally, some conclusions are drawn in Section VII.

II. The Class of Time-Variant Systems

The classes of time-variant systems considered in this paper are defined via the time-variant frequency response function. Therefore, we first briefly recall the definition of the time-variant frequency response function and its properties (Section II-A), before introducing the classes of slowly time-variant (Section II-B) and nonlinear slowly time-variant (Section II-C) systems.

A. The Time-Variant Frequency Response Function

A linear time-variant (LTV) system is uniquely characterized by its time-variant impulse response $g(t,\tau)$. The latter describes the response of the system as a function of the time t when a Dirac impulse excitation is applied at time instant τ. The time-variant frequency response function (TV-FRF) $G(j\omega,t)$ is related to the time-variant impulse response $g(t,\tau)$ as

$$G\left(j\omega,t\right)=\int_{-\infty}^{+\infty}g\left(t,t-\tau\right)e^{-j\omega\tau}d\tau \tag{1}$$

For causal systems the time-variant impulse response satisfies $g(t,\tau)=0$ if $t<\tau$, and the lower integration boundary in (1) is replaced by zero. In [6], [7] it is shown that the properties of the TV-FRF (1) are similar to those of an FRF of a linear time-invariant (LTI) system: (i) the steady state response to $u(t)=\sin(\omega_0 t)$ is the amplitude and phase modulated signal $y_0(t)=|G(j\omega_0,t)|\sin(\omega_0 t+\angle G(j\omega_0,t))$; and (ii) the transient response to an arbitrary excitation $u(t)$ is calculated as $y_0(t)=L^{-1}\{G(s,t)U(s)\}$, with $U(s)$ the Laplace transform of $u(t)$ and $L^{-1}\{\}$ the inverse Laplace transform operator.

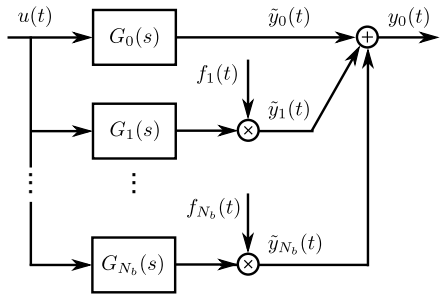

Figure 1. Direct model of a linear time-variant system. The time-variation is modeled by the known basis functions $f_p(t)$, $p=1,2,\ldots,N_b$.

Given a complete set of basis functions $f_p(t)$, $p=0,1,\ldots$, over the interval $[0,T]$, the TV-FRF (1) can be expanded in series as

$$G\left(j\omega,t\right)=\sum_{p=0}^{\infty}G_p\left(j\omega\right)f_p\left(t\right)\quad\forall\, t\in[0,T] \tag{2}$$

where the frequency dependent coefficients $G_p(j\omega)$ represent FRFs of LTI systems. Without any loss in generality, the following constraints can be imposed on the basis functions

$$f_0\left(t\right)=1\ \text{ and }\ \frac{1}{T}\int_0^T f_p\left(t\right)dt=0\ \text{ for }\ p>0 \tag{3}$$

In this paper we consider arbitrarily time-varying systems and, hence, choose an orthogonal polynomial basis (Legendre polynomials) to describe the time-variation.

B. Linear Slowly Time-Variant Systems

Note that the series expansion (2) contains infinitely many FRFs, which is unpractical for nonparametric estimation. Therefore, we limit ourselves to the class of time-variant systems whose TV-FRF can be expanded in a finite sum.

Definition 1. The class of slowly time-variant systems considered includes all time-variant systems whose time-variant frequency response function can be written as

$$G\left(j\omega,t\right)=\sum_{p=0}^{N_b}G_p\left(j\omega\right)f_p\left(t\right)\quad\forall\, t\in[0,T] \tag{4}$$

where $f_p(t)=P_p(2t/T-1)$, with $P_p(x)$ the Legendre polynomial of degree p, see [21].

Note that $f_p(t)=P_p(2t/T-1)$ satisfies the constraints (3). Figure 1 shows the block diagram corresponding to the slowly time-variant system (4) (proof: apply $y_0(t)=L^{-1}\{G(s,t)U(s)\}$). It is called the direct model of the time-variant system in the sequel of this paper.

The term "slowly time-variant" in Definition 1 is justified by the fact that the bandwidth of the Legendre polynomials is concentrated around DC. It does not exclude that the time-variation can be strong (large). The latter is the case if the amplitude of at least one $G_p(j\omega)$, $p>0$, is not much smaller

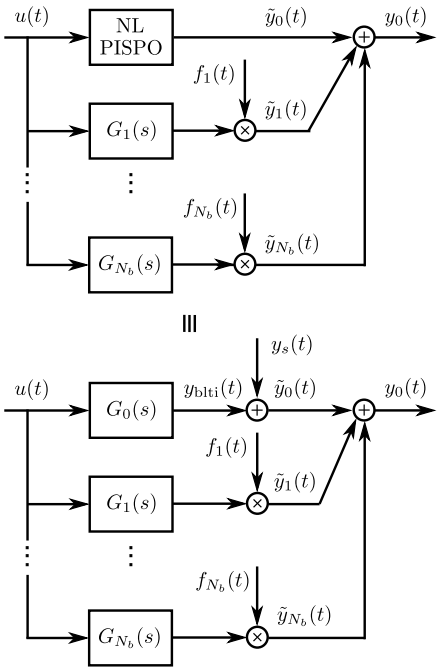

Figure 2. Direct model of a particular class of nonlinear slowly time-variant systems: the steady state response of the nonlinear time-invariant sub-system to a periodic input is periodic with the same period as the input (= nonlinear period in, same period out system). $G_0(s)$ represents the best linear approximation of the nonlinear period in, same period out (NL PISPO) sub-system, and the best linear time-invariant approximation of the overall nonlinear time-variant system. The stochastic nonlinear distortion $y_s(t)$ is uncorrelated with – but not independent of – the input $u(t)$.

than that of $G_0(j\omega)$. If for all $p > 0$ $|G_p(j\omega)| \ll |G_0(j\omega)|$, then the time-variation is weak (small).

C. Nonlinear Slowly Time-Variant Systems

We assume here that only the time-invariant branch in Fig. 1 behaves nonlinearly (see Fig. 2, top block diagram) and that it belongs to the class of PISPO (period in, same period out) nonlinear systems. The class of PISPO nonlinear systems includes all nonlinear systems whose response can be approximated arbitrarily well in mean square sense by a Volterra series on a given input domain. It has the property that the steady state response to a periodic input is periodic with the same period as the input, and comprises hard nonlinearities such as saturation and discontinuities [22]. Chaos and sub-harmonics are excluded.

Definition 2. The class of nonlinear slowly time-variant systems considered includes all nonlinear time-variant systems whose response can be written as the sum of the response to a PISPO nonlinear time-invariant system and the response to a linear slowly time-variant system (Definition 1).

For a given class of random excitation signals with the same power spectral density and probability density function, the response of the PISPO nonlinear system in the top block diagram of Fig. 2 can be written as the sum of the response to the best (in mean square sense) linear approximation $G_0(s)$ and the stochastic nonlinear distortion $y_s(t)$ (see Fig. 2, bottom block diagram). The latter is uncorrelated with – but not independent of – the input $u(t)$ [23], [24]. Hence, (4) is the best (in mean square sense) linear time-variant approximation of the nonlinear slowly time-variant system.

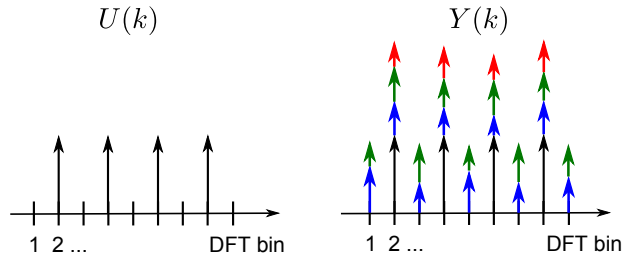

Figure 3. Noisy response of a nonlinear slowly time-variant system to a periodic excitation. The left plot shows the input DFT spectrum $U(k) = \text{DFT}(u(t))$ of two consecutive periods of the periodic excitation. The right plot shows the output DFT spectrum $Y(k) = \text{DFT}(y(t))$ of the corresponding noisy response $y(t) = y_{\text{blti}}(t) + y_s(t) + n_y(t)$: output of the best linear time-invariant approximation $y_{\text{blti}}(t)$ (black arrows); nonlinear distortions $y_s(t)$ (red arrows); time-variant contributions $y_{\text{TV}}(t)$ (blue arrows); and disturbing noise $n_y(t)$ (green arrows).

III. The Class of Excitation Signals

A. Definition

A random phase multisine is the sum of harmonically related sinewaves

$$u(t) = \frac{1}{\sqrt{F}} \sum_{k=k_1}^{k_2} A_k \sin(2\pi k f_0 t + \phi_k) \tag{5}$$

with $A_k \geqslant 0$ the user defined amplitudes, ϕ_k the random phases chosen such that $\mathbb{E}\{e^{j\phi_k}\} = 0$, $k_1, k_2 \in \mathbb{N}_0$, and F the number of non-zero amplitudes ($F = \text{ord}\{A_k,\ k = k_1, k_1+1, \ldots, k_2 \mid A_k > 0\}$). The amplitudes A_k in (5) are divided by $\sqrt{F}$ such that the signal rms value is independent of the number of sinewaves F.

Note that (5) belongs to the class of Gaussian excitation signals with a given (Riemann equivalent) power spectrum [25]. Note also that periodic excitations are needed to distinguish the disturbing noise from the nonlinear distortions (see Section III-B and [22]).

B. Noisy Response of a Nonlinear Slowly Time-Variant System to a Periodic Input

Consider a periodic excitation signal $u(t)$ and its corresponding discrete Fourier transform (DFT) $U(k) = \text{DFT}(u(t))$,

$$U(k) = \frac{1}{\sqrt{N}} \sum_{n=0}^{N-1} u(nT_s)\, e^{-j2\pi kn/N} \tag{6}$$

with T_s the sample period and N the number of time domain samples. The DFT (6) of P consecutive signal periods of $u(t)$ has the following property

$$U(mP + r) = 0 \tag{7}$$

for $r = 1, 2, \ldots, P-1$ and $m = 0, 1, \ldots, N/P-1$, with $N/P \in \mathbb{N}_0$ the number of samples per period. Hence, signal energy can only be present at DFT bins mP, $m = 0, 1, \ldots, N/P-1$. The left plot of Fig. 3 shows the case $P = 2$.

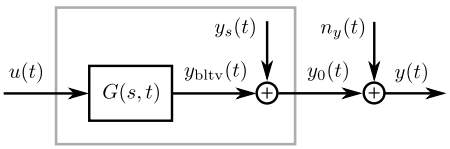

Figure 4. Noisy output observation $y(t)$ of the response $y_0(t)$ of a nonlinear slowly time-variant system (grey box) to a known random phase multisine excitation $u(t)$. $G(s,t)$ is the best linear time-variant approximation satisfying (4), $y_{\mathrm{bltv}}(t)$ the output of the best linear time-variant approximation, $y_s(t)$ the stochastic nonlinear distortion that is uncorrelated with – but not independent of – the input $u(t)$, and $n_y(t)$ the stationary output disturbance.

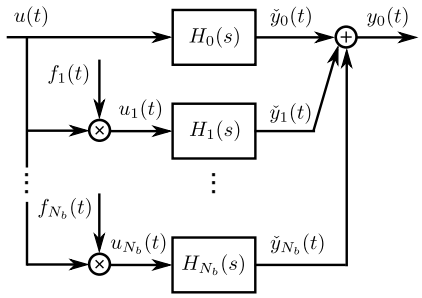

Figure 5. Indirect model of a linear slowly time-variant system.

The steady state response of a nonlinear slowly time-variant system (see Definition 2) to a periodic input can be split into a periodic nonlinear time-invariant part $\tilde{y}_0(t) = y_{\mathrm{blti}}(t) + y_s(t)$ and a non-periodic linear time-variant part $y_{\mathrm{TV}}(t) = \sum_{p=1}^{N_b} \tilde{y}_p(t)$ (see Fig. 2). While $y_{\mathrm{TV}}(t)$ contains signal energy at all DFT bins (see Fig. 3, right plot, blue arrows), $\tilde{y}_0(t)$ contains signal energy at DFT bins mP, $m = 0, 1, \ldots, N/P - 1$ only. The latter is the sum of the response of the best linear time-invariant approximation $y_{\mathrm{blti}}(t)$ (see Fig. 3, right plot, black arrows) and the nonlinear distortion $y_s(t)$ (see Fig. 3, right plot, red arrows). Finally, a filtered white noise output disturbance $n_y(t)$ contains noise energy at all DFT bins (see Fig. 3, right plot, green arrows).

The fact that the nonlinear distortion $y_s(t)$ is zero at DFT bins $mP + r$, $r = 1, 2, \ldots, P - 1$ and $m = 0, 1, \ldots, N/P - 1$, is the key property that allows us to distinguish the noise from the nonlinear distortion (see Section V-B).

Note that under non-steady state conditions, an additional transient (leakage) term affects the output DFT spectrum $Y(k)$ that cannot be distinguished from the spectral leakage of the non-periodic time-variant contributions $y_{\mathrm{TV}}(t)$ (see also Section V-A).

IV. Assumptions

We list here the assumptions concerning the time-variant system, the excitation signal, the experimental setup, and the disturbing output noise (see also Fig. 4):

1) The time-variant system belongs to the class of nonlinear slowly time-variant systems (Definition 2).
2) The excitation $u(t)$ is a random phase multisine (5) and is known exactly.
3) An integer number $P \geqslant 2$ of signal periods $T_0 = 1/f_0$ of the (transient) response is measured.
4) The output measurements are disturbed by additive, stationary, discrete- or continuous-time, filtered (band-limited) white noise $n_y(t)$.

Assumption 1 is an approximation which is reasonable for weakly nonlinear, slowly time-variant systems with small time-variation (see Section VI). Assumption 3 is a hardware requirement called coherent sampling: the arbitrary waveform generator and the data acquisition channels must be synchronized such that $f_0 = f_s P/N$, with $f_s = 1/T_s$ the sample frequency and N/P the number of samples per period. This condition is easily fulfilled in practice: either the generator clock is used as external clock for the acquisition unit, or the generator and acquisition clocks originate from the same mother clock (e.g., VXI[1] and PXI[2] based instrumentation). Assumption 4 is also an approximation because the process noise generated by a time-variant system is likely to be non-stationary. However, for slowly time-variant systems the non-stationary noise can be approximated very well by its best linear stationary approximation [26].

V. Nonparametric Estimation Procedure

Based on the indirect model of a slowly time-variant system described in Section V-A and generalizing the results of [16], [19], [20], an indirect nonparametric estimation method for the time-variant frequency response function (4) is developed in Section V-B. Finally, the bias error of the estimate is analyzed in Section V-C.

A. The Indirect Model of a Slowly Time-Variant System

In [16] it has been proven that the direct model of a slowly time-variant system shown in Fig. 1 can be transformed into an equivalent indirect model shown in Fig. 5, with the following relationship between the dynamics

$$G_r(s) = H_r(s) + \frac{2}{T}(2r+1) \sum_{i=0}^{\left\lfloor \frac{N_b - r - 1}{2} \right\rfloor} H^{(1)}_{2i+1+r}(s) + \frac{4}{T^2} \sum_{i=1}^{\left\lfloor \frac{N_b - r}{2} \right\rfloor} \beta_{2i,r} H^{(2)}_{2i+r}(s) + O\left(T^{-3}\right) \tag{8}$$

where $\lfloor x \rfloor$ is the largest integer smaller than or equal to x, $H_r^{(m)}(s)$ the m-th order derivative of $H_r(s)$ w.r.t. s, $\beta_{2i,r}$ the following coefficients

$$\begin{aligned} \beta_{2i,r} &= \gamma_r + \delta_r(i-1) + \mu_r(i-1)^2 \\ \gamma_r &= 1.5 + 4r + 2r^2 \\ \delta_r &= 2.5 + 6r + 2r^2 \\ \mu_r &= 1 + 2r \end{aligned} \tag{9}$$

and where $O(T^{-n})$ with $n > 0$ means that $\lim_{T\to\infty} T^n O(T^{-n}) < \infty$. The $O\left(T^{-3}\right)$ bias term in (8) depends on the higher order derivatives $H_q^{(m)}(s)$, with $N_b \geqslant q \geqslant r + 3$, and where m ranges from

[1]VXI is an open bus standard and stands for VME eXtensions for Instrumentation

[2]PXI is an open bus standard and stands for PCI eXtensions for Instrumentation

$3 + (q + 1 + r) \bmod 2$ to $q - r$ in steps of 2 (mod stands for modulo).

There is an important conceptual difference between the direct (Fig. 1) and indirect (Fig. 5) models. Indeed, while the identification of the direct model requires single-input $u(t)$, single-output $y(t)$ linear time-variant estimation techniques [15], the indirect model can be identified using algorithms for multiple-input $u(t), u_1(t), \ldots, u_{N_b}(t)$, single-output $y(t)$ linear time-invariant systems (the inputs $u_p(t) = f_p(t)u(t)$ are known). The transfer functions $G_p(s)$ are then recovered from $H_p(s)$ via (8).

The noiseless input-output DFT spectra of the indirect model of a linear slowly time-variant system are related as

$$Y_0(k) = \sum_{p=0}^{N_b} H_p(j\omega_k) U_p(k) + T_H(j\omega_k) \tag{10}$$

with $Y_0(k) = \mathrm{DFT}(y_0(t))$, $U_p(k) = \mathrm{DFT}(u(t)f_p(t))$, $U_0(k) = U(k)$ ($f_0(t) = 1$), and $T_H(j\omega)$ a rational function of $j\omega$. For nonlinear slowly time-variant systems (Definition 2), the DFT spectrum $Y_S(k)$ of the nonlinear distortion $y_s(t)$ is added to the right hand side of (10) (proof: apply the indirect model to the bottom block diagram of Fig. 2).

Note that under non-steady state conditions $T_H(j\omega_k)$ in (10) also depends on the leakage term of the time-invariant branch in Fig. 5. However, this does not affect the estimation of the dynamics $H_p(j\omega_k)$, $p = 1, 2, \ldots, N_b$, in the time-variant branches.

B. The Indirect Method

Following the same lines of Section III-B, it can be seen that the DFT spectrum of P consecutive signal periods of $\check{y}_0(t)$ in the indirect model (see Fig. 5) is zero at DFT bins $mP + r$ for $r = 1, 2, \ldots, P - 1$ and $m = 0, 1, \ldots, N/P - 1$; while $\sum_{p=1}^{N_b} \check{y}_p(t)$ contains signal energy at all DFT bins. Hence, the right plot of Fig. 3 remains valid for the response of the indirect model: the black arrows represent $\check{y}_0(t)$ and the blue arrows stand for $\sum_{p=1}^{N_b} \check{y}_p(t)$. This observation results in the three-step procedure discussed in detail in the sequel. Using the non-excited DFT bins the FRFs in the time-variant branches of the indirect model and their noise variances are estimated in the first step. In step 2 the contribution of the time-variant branches is subtracted from the output at the excited DFT bins. What remains is the output of the time-invariant branch whose dynamics and total variance (= sum noise variance and variance nonlinear distortions) are estimated. Finally, the indirect model is converted to the direct model in step 3.

Step 1 – From (10) it follows that the known input, noisy output DFT spectra evaluated at the non-excited DFT bins $k = mP + r$, with $r = 1, 2, \ldots, P - 1$ and $m = 0, 1, \ldots, N/P - 1$, satisfy

$$Y(k) = \sum_{p=1}^{N_b} H_p(j\omega_k) U_p(k) + T_H(j\omega_k) + N_Y(k) \tag{11}$$

with $N_Y(k) = \mathrm{DFT}(n_y(t))$. Using (11), the FRFs $H_p(j\omega_k)$, $p = 1, 2, \ldots, N_b$, the transient term $T_H(j\omega_k)$, and their noise covariances are estimated nonparametrically at the excited DFT bins $k = mP$ via the local polynomial method (LPM) for arbitrary excitations with a given number of degrees of freedom dof^{noise} [27]. The latter quantifies the difference between the local number of equations (non-excited frequencies) and the local number of parameters in the linear least squares estimate of the FRFs and the transient term. Note that the number N_b of time-variant branches is unknown and is also estimated from the data: start with $N_b = 1$ and increase its value until the estimate $\hat{H}_r(j\omega_k)$ is of the same order of magnitude as its standard deviation for all values of k and for all $r \geqslant N_b$. $N_b - 1$ is then the significant number of time-varying branches.

Step 2 – Using the estimates obtained in Step 1, the response of the time-variant branches and the leakage term are subtracted from the output at the excited DFT bins $k = mP$

$$Y(k) - \sum_{p=1}^{N_b} \hat{H}_p(j\omega_k) U_p(k) - \hat{T}_H(j\omega_k) \tag{12}$$

giving a nonparametric estimate of the response $\check{Y}_0(k) = \mathrm{DFT}(\check{y}_0(t))$ of the time-invariant branch in Fig. 5 that is disturbed by noise and nonlinear distortion. From the residual (12), the FRF $H_0(j\omega_k)$ and its total variance (= sum noise variance and variance nonlinear distortion) are estimated nonparametrically following the same lines of the local polynomial method (LPM) for periodic excitations with a given number of degrees of freedom dof [28]. The latter quantifies the difference between the local number of equations (excited frequencies) and the local number of parameters in the linear least squares estimate of $H_0(j\omega_k)$. Using the noise covariances obtained in Step 1, the noise variance of $\hat{H}_0(j\omega_k)$ is calculated. Comparison of the noise variance with the total variance quantifies the variance of the stochastic nonlinear distortions $Y_S(k) = \mathrm{DFT}(y_s(t))$.

Step 3 – Finally, following the same lines of [19], nonparametric estimates $\hat{G}_p(j\omega_k)$, $p = 0, 1, \ldots, N_b$, and their noise and total variances are obtained via (8), where the first and second order derivatives $H_r^{(n)}(j\omega_k)$, $n = 1, 2$, are approximated numerically by (non-)central differences

$$H_r^{(1)}(j\omega_k) = \sum_{i=-1}^{+1} w_{1,k_i} H_r(j\omega_{k_i}) + O\left(T^{-2}\right) \tag{13}$$

$$H_r^{(2)}(j\omega_k) = \sum_{i=-1}^{+1} w_{2,k_i} H_r(j\omega_{k_i}) + O\left(T^{-1}\right) \tag{14}$$

(see [20], [29]) with $k_0 = k$, and where the weights w_{1,k_i} and w_{2,k_i} are calculated as

$$
\begin{aligned}
w_{1,k_{-1}} &= \frac{j\omega_{k_1} - j\omega_k}{\left(j\omega_{k_{-1}} - j\omega_k\right)\left(j\omega_{k_1} - j\omega_{k_{-1}}\right)} \\
w_{1,k} &= \frac{-j\omega_{k_{-1}} + 2j\omega_k - j\omega_{k_1}}{\left(j\omega_{k_{-1}} - j\omega_k\right)\left(j\omega_{k_1} - j\omega_k\right)} \\
w_{1,k_1} &= \frac{j\omega_k - j\omega_{k_{-1}}}{\left(j\omega_{k_1} - j\omega_k\right)\left(j\omega_{k_1} - j\omega_{k_{-1}}\right)} \\
w_{2,k_{-1}} &= \frac{2}{\left(j\omega_{k_{-1}} - j\omega_k\right)\left(j\omega_{k_{-1}} - j\omega_{k_1}\right)} \\
w_{2,k} &= \frac{2}{\left(j\omega_k - j\omega_{k_{-1}}\right)\left(j\omega_k - j\omega_{k_1}\right)} \\
w_{2,k_1} &= \frac{2}{\left(j\omega_{k_1} - j\omega_{k_{-1}}\right)\left(j\omega_{k_1} - j\omega_k\right)}
\end{aligned}
$$

Note that for uniformly distributed excited harmonics, the non-central differences (13) and (14) simplify to the central differences and the $O(T^{-1})$ bias in (14) becomes an $O(T^{-2})$ [31].

C. Bias Error

Since the (non-)central differences (13) and (14) equal the true derivatives within a bias error of, respectively, an $O(T^{-2})$ and $O(T^{-1})$, and since the bias error of the LPM estimates $\hat{H}_p(j\omega_k)$, $p = 0, 1, \ldots, N_b$, is an $O\left(T^{-(R+1)}\right)$, with $R \geqslant 2$ the order of the local polynomial approximations of $H_p(j\omega)$ and $T_H(j\omega)$ [22], [27]; the bias on $\hat{G}_p(j\omega_k)$, $p = 0, 1, \ldots, N_b$, is an $O(T^{-3})$ (proof: combine (8), (13), and (14)).

If a simplified estimate of $G_p(j\omega_k)$, $p = 0, 1, \ldots, N_b$, is calculated as

$$
\hat{G}_r(s) = \hat{H}_r(s) + \frac{2}{T}(2r+1) \sum_{i=0}^{\left\lfloor \frac{N_b - r - 1}{2} \right\rfloor} \hat{H}^{(1)}_{2i+1+r}(s) \qquad (15)
$$

then the resulting $O(T^{-2})$ bias can be estimated as

$$
\mathbb{E}\left\{\hat{G}_r(j\omega_k)\right\} - G_r(j\omega_k) \approx \frac{4}{T^2} \sum_{i=1}^{\left\lfloor \frac{N_b - r}{2} \right\rfloor} \beta_{2i,r} \hat{H}^{(2)}_{2i+r}(s) \qquad (16)
$$

(proof: use (8), (13), and (14)). Note that approximation (15) is useful if its variance is larger than its bias (16); a condition that can easily be verified.

VI. Illustration on a Time-Variant Electronic Circuit

Although the indirect method described in Section V-B has extensively been verified on simulations examples satisfying the assumptions of Section IV (see, for example, [30]), we prefer to report the results of a measurement example where the conditions of Section IV have not been imposed by construction.

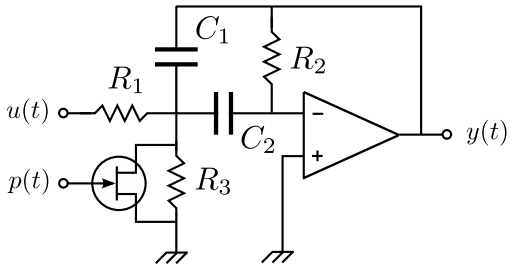

Figure 6. Time-variant second order bandpass filter consisting of a high gain operational amplifier (CA741CE), a JFET transistor (BF245B) with gate voltage $p(t)$, three resistors ($R_1 = R_2 = 10\,\mathrm{k}\Omega$ and $R_3 = 470\,\mathrm{k}\Omega$), and two capacitors ($C_1 = C_2 = 10\,\mathrm{nF}$). The electronic circuit is excited by a random phase multisine and $P = 4$ multisine periods of the input $u(t)$ and output $y(t)$ signals are measured.

A. Measurement Setup

The device under test is a second order bandpass filter whose pole position is modified by the gate voltage $p(t)$ of a JFET transistor (see Fig. 6). This bandpass filter is a linear parameter varying circuit with parameter $p(t)$. However, since the gate voltage $p(t)$ is not used in the estimation procedure, the device under test acts as a linear time-variant circuit. A random phase multisine excitation $u(t)$ consisting of $F = 8347$ harmonics uniformly distributed in the band $[200.27\,\mathrm{Hz}, 39.997\,\mathrm{kHz}]$ (Eq. (5) with $k_1 = 42$, $k_2 = 8388$, and $f_0 = 4.7684\,\mathrm{Hz}$), constant amplitudes A_k, and uniformly $[0, 2\pi)$ distributed random phases ϕ_k, is applied to the electronic circuit. During the experiment, the gate voltage changes as

$$
p(t) = p_0 + p_1((t/T)^3 - t/T) \qquad (17)
$$

with $T = 4/f_0$ the experiment duration. Experiments are performed for three different input rms values 92 mV, 184 mV, and 368 mV (three different choices of the constant A_k's in (5)) and five different peak-to-peak variations of the gate voltage 50 mV, 197 mV, 295 mV, 392 mV, and 589 mV (five different choices of p_0 and p_1 in (17); see Fig. 7).

The generator (HP E1445A) and data acquisition (HP E1430A) cards of the VXI measurement setup are synchronized (coherent sampling: $f_0 = f_s P/N$, with $f_s = 156.25\,\mathrm{kHz}$ the sampling frequency, $N/P = 32768$ the number of samples per signal period, and N the total number of acquired samples per signal), and four periods ($P = 4$) of the steady state response are measured for each of the three input rms values and each of the five peak-to-peak gate voltage values. To reach steady state, the generation is started before the acquisition and 5 periods are measured of which the first is removed. To avoid loading of the electronic circuit, voltage buffers ($Z_{\mathrm{in}} > 5\,\mathrm{M}\Omega$, $Z_{\mathrm{out}} = 50\,\Omega$) are put in front of the data acquisition channels ($Z_{\mathrm{in}} = 50\,\Omega$).

B. Results

All LPM estimates (see Section V-B) are performed with the following settings: a fourth order ($R = 4$) local polynomial approximation of the FRFs and the leakage term in Steps 1 and 2, $dof^{\mathrm{noise}} = 200$ in Step 1, and $dof = 5$ in Step 2. For increasing peak-to-peak variation of the gate voltage $p(t)$, the significant number of time-variant branches in (4) equals

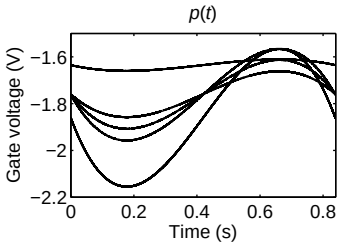

Figure 7. Variation of the gate voltage during the experiment. The gate voltage is of the form $p(t) = p_0 + p_1((t/T)^3 - t/T)$, with T the experiment duration (4 multisine periods). The peak-to-peak variation of the five different gate voltages are, respectively, 50 mV, 197 mV, 295 mV, 392 mV, and 589 mV.

$N_b = 6$, 7, 8, 9, and 10 for all input rms values. The results are shown in Figures 8–10.

Fig. 8 shows the estimates of the direct model (4) for the smallest peak-to-peak variation of the gate voltage and all input rms values. It can be seen that for increasing input rms values, the signal-to-noise ratio (SNR) of the estimates increases (light green to dark green lines in all plots), while the signal-to-distortion ratio (SDR) decreases (light pink to red lines in the top left plot). Hence, for the smallest peak-to-peak variation of the gate voltage the hypothesis that the output can be split into a nonlinear time-invariant part and a linear time-variant part (see Definition 2) is fulfilled. This is no longer true for all other peak-to-peak variations of the gate voltage, which is illustrated in Fig. 9 for $p(t) = 392\,\mathrm{mV_{pp}}$. Indeed, it can be seen from Fig. 9 that for increasing input rms values the SNR of the estimates (light green to green lines in all plots) increases in the band $[22\,\mathrm{kHz}, 40\,\mathrm{kHz}]$ while it decreases in the band $[200\,\mathrm{Hz}, 22\,\mathrm{kHz}]$; a phenomenon that can only be explained by the nonlinear behavior of the time-variant branches in that frequency band. This is consistent with the observation that the time-variants effects are the largest in the band $[200\,\mathrm{Hz}, 22\,\mathrm{kHz}]$ (see Fig. 9, FRFs $G_p(j\omega)$, $p = 1, 3, 4, \ldots, 9$). Although the time-variant electronic circuit does not satisfy Definition 2 for the larger peak-to-peak variations of the gate voltage, the nonlinear behavior is still detected (the light pink/red lines are still well above the light green/green lines in the top left plot) and the difference between the total (light pink to red lines) and the noise (light green to green lines) variances of $\hat{G}_0(j\omega_k)$ is now a lower bound for the variance of the nonlinear distortion $Y_S(k)$.

Note that $\hat{G}_2(j\omega_k) = 0$ for all input rms values and peak-to-peak variations of the gate voltage (see, for example, Figs. 8 and 9). This can be explained as follows. The time-variant FRF $G(j\omega, t)$ depends on the time t via the gate voltage $p(t)$, viz. $G(j\omega, t) = \tilde{G}(j\omega, p(t))$. First order Taylor series expansion of $\tilde{G}(j\omega, p(t))$ w.r.t. $p(t)$ gives

$$\tilde{G}(j\omega, p(t)) \approx \tilde{G}_0(j\omega) + \tilde{G}_1(j\omega)p(t) \tag{18}$$

Combining (17) and (18) shows that $G(j\omega, t)$ (4) does not depend on t^2 which implies that $G_2(j\omega) = 0$.

Finally, using the nonparametric FRF estimates $\hat{G}_p(j\omega_k)$, $p = 0, 1, \ldots, N_b$, a three dimensional plot of the time-variant FRF $G(j\omega, t)$ (4) can be drawn. Fig. 10 shows the corresponding

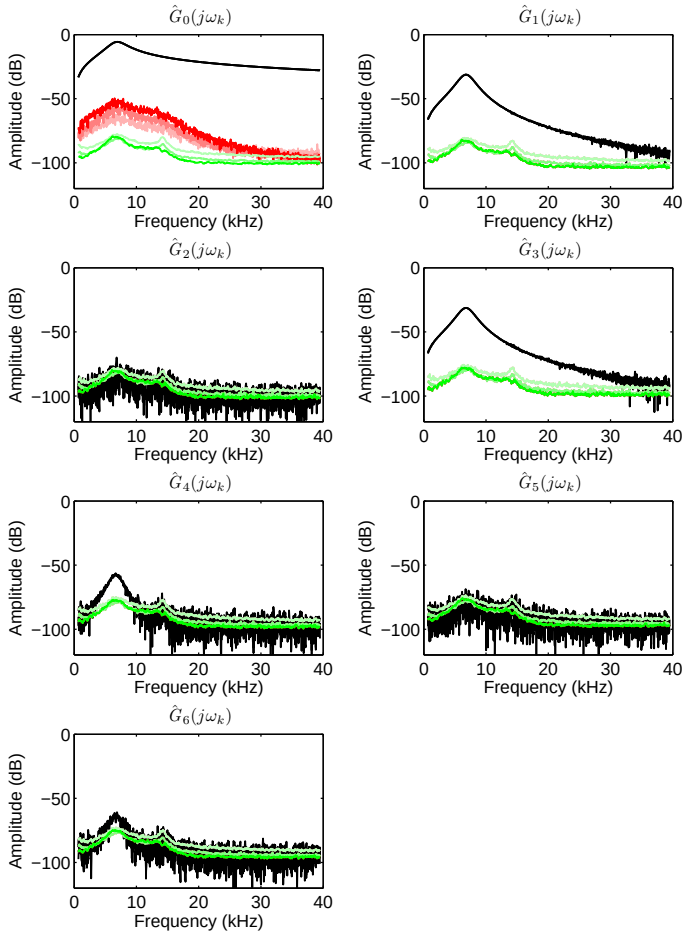

Figure 8. Nonparametric estimates of the FRFs in the direct model (4) for increasing input rms values (92 mV, 184 mV, and 368 mV) and 50 mV peak-to-peak variation of the gate voltage. Black lines: the estimated FRFs $\hat{G}_p(j\omega)$, $p = 0, 1, \ldots, 6$; light green to dark green lines: noise variance FRF estimates for increasing input rms values; and light pink to red lines: total variance FRF estimates for increasing input rms values.

frequency-time plots for an input rms value of 368 mV and increasing peak-to-peak variation of the gate voltage (from top to bottom). As expected, there is a large similarity between the time-dependency of the time-variant FRFs at the resonance frequency in Fig. 10 and the gate voltages in Fig. 7.

VII. Conclusions

An indirect estimation procedure has been presented for detecting and quantifying the noise level and the level of the nonlinear distortions in time-variant frequency response function (TV-FRF) measurements using random phase multisine excitations. The proposed method is nonparametric in the dynamics and parametric in the arbitrary time-variation, and only requires estimation tools developed for multiple-input, single-output linear time-invariant systems.

If the actual response of the nonlinear time-variant system can be split into a nonlinear time-invariant part and a linear time-variant part, then the quantification of the nonlinear distortion is exact, otherwise it is a lower bound for the true value. In the former case the estimated TV-FRF is the best (in mean square

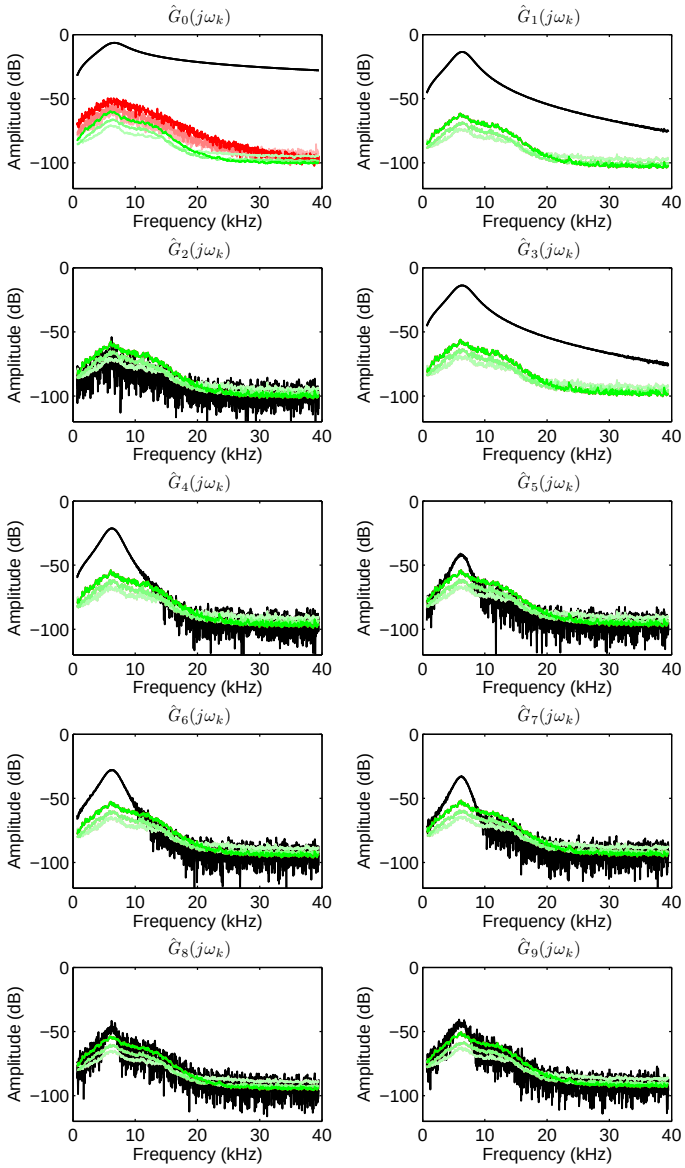

Figure 9. Nonparametric estimates of the FRFs in the direct model (4) for increasing input rms values (92 mV, 184 mV, and 368 mV) and 392 mV peak-to-peak variation of the gate voltage. Black lines: the estimated FRFs $\hat{G}_p(j\omega)$, $p = 0, 1, \ldots, 9$; light green to dark green lines: noise variance FRF estimates for increasing input rms values; and light pink to red lines: total variance FRF estimates for increasing input rms values.

sense) linear time-variant approximation of the nonlinear time-variant system.

Acknowledgements

This work is sponsored by the Research Council of the Vrije Universiteit Brussel, the Research Foundation Flanders (FWO-Vlaanderen), the Flemisch Government (Methusalem Fund METH1), and the Belgian Federal Government (Interuniversity Attraction Poles programme IAP VII DYSCO).

References

[1] Van Ingelgem, Y., Tourwé, E., Vereecken, J. and Hubin, A., "Application of multisine impedance spectroscopy, FE-AES and FE-SEM to study the early stages of copper corrosion," *Electrochemica Acta*, vol. 53, no. 25, pp. 7523-7530, 2008.

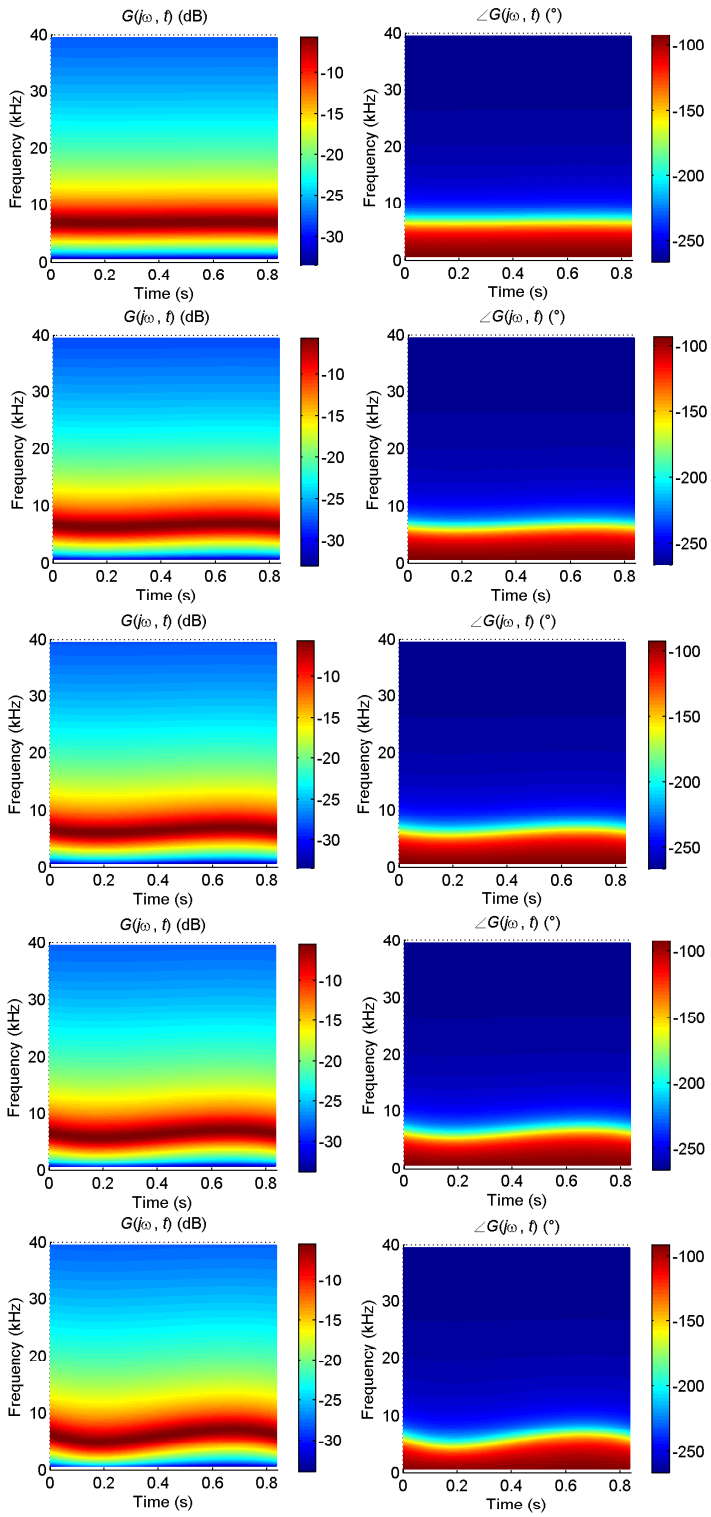

Figure 10. Frequency-time plots of the amplitude (left column) and phase (right column) of the time-variant FRF for increasing peak-to-peak variation of the gate voltage (from top to bottom: 50 mV, 197 mV, 295 mV, 392 mV, and 589 mV) and 368 mV input rms value.

[2] Chen, S. Y., and Yuan, J. S., "Adaptive gate bias for power amplifier temperature compensation," *IEEE Trans. on Device and Material Reliability*, vol. 11, no. 3, pp. 442-449, 2011.

[3] Aerts, J. R. M. and Dirckx, J. J. J., "Nonlinearity in eardrum vibration as a function of frequency and sound pressure," *Hearing Research*, vol. 263, no. 1-2, pp. 26-32, 2010.

[4] Dimitriadis, G. and Cooper, J. E., "Flutter prediction from flight flutter test data," *Journal of Aircraft*, vol. 38, no. 2, pp. 355-367, 2001.

[5] Pop, V., Bergveld, H. J., Notten, P. H. L., and Regtien, P. P. L., "State-of-the-art of battery state-of-charge determination," *Measurement Science & Technology*, vol. 16, no. 12, pp. R93-R110, 2005.

[6] Zadeh, L. A., "The determination of the impulsive response of variable networks," *Journal of Applied Physics*, vol. 21, pp. 642-645, 1950.

[7] Zadeh, L. A., "Frequency analysis of variable networks," *Proceedings of the I.R.E.*, vol. 38, pp. 291-299, 1950.

[8] Aguilera, R. P., Godoy, B. I., Agüero, J. C., Goodwin, G. C., and Yuz, J. I., "An EM-based identification algorithm for a class of hybrid systems with application to power electronics," *International Journal of Control*, vol. 87, no. 7, pp. 1339-1351, 2014.

[9] Hamilton, J. D., "Analysis of time series subject to changes in regime," *Journal of Econometrics*, vol. 45, no. 1-2, pp. 39-70, 1990.

[10] Yin, G. G., Kan, S., Wang, L. Y., and Xu, C. Z., "Identification of systems with regime switching and unmodeled dynamics," *IEEE Trans. Autom. Contr.*, vol. 54, no. 1, pp. 34-47, 2009.

[11] Paoletti, S., Juloski, A. Lj., Ferrari-Trecate, G., and Vidal, R., "Identification of hybrid systems – A tutorial," *European Journal of Control*, vol. 13, no. 2-3, pp. 242-260, 2007.

[12] Louarroudi, E., Pintelon, R. and Lataire, J., "Nonparametric tracking of the time-varying dynamics of weakly nonlinear periodically time-varying systems using periodic inputs," *IEEE Trans. Instrum. and Meas.*, vol. 61, no. 5, pp. 1384-1394, 2012.

[13] Sams, A. D. and Marmarelis, V. Z., "Identification of linear periodically time-varying systems using white-noise test inputs," *Automatica*, vol. 24, no. 4, pp. 563-567, 1988.

[14] Sanchez, B., Fernandez, X., Reig, S., and Bragos, R., "An FPGA-based frequency response analyzer for multisine and stepped sine measurements on stationary and time-varying impedance," *Measurement Science & Technology*, vol. 25, no. 1, 015501, 2014 (doi 10.1088/0957-0233/25/1/015501).

[15] Lataire, J., Pintelon, R., and Louarroudi, E., "Non-parametric estimate of the system function of a time-varying system," *Automatica*, vol. 48, no. 4, pp. 666-672, 2012.

[16] Pintelon, R., Louarroudi, E., and Lataire, J., "Nonparametric time-variant frequency response function estimates using arbitrary excitations," *Automatica*, vol. 51, no. 1, pp. 308-317, 2015.

[17] Spiridonakos, M. D. and Fassois, S. D., "Parametric identification of a time-varying structure based on vector vibration response measurements," *Mechanical Systems and Signal Processing*, vol. 23, no. 6, pp. 2029-2048, 2009.

[18] Sanchez, B., Louarroudi, E., Bragos, R., and Pintelon R., "Harmonic impedance spectra identification from time-varying bioimpedance: theory and validation," *Physiological Measurement*, vol. 34, no. 10, pp. 1217-1238, 2013.

[19] Pintelon, R., Louarroudi, E., and Lataire, J., "Detecting and quantifying the nonlinear and time-variant effects in FRF measurements using periodic excitations," *IEEE Trans. Instrum. and Meas.*, vol. 62, no. 12, pp. 3361-3373, 2013.

[20] Pintelon, R., Louarroudi, E., and Lataire, J., "Quantifying the time-variation in FRF measurements using random phase multisines with non-uniformly spaced harmonics," *IEEE Trans. Instrum. and Meas.*, vol. 63, no. 5, pp. 1384-1394, 2014.

[21] Abramowitz, M. and Stegun, I. A., *Handbook of Mathematical Functions*. New York: Dover Publications, 1970.

[22] Pintelon, R., and Schoukens, J., *System Identification: A Frequency Domain Approach*. 2nd edition, Hoboken (USA): Wiley – IEEE Press, 2012.

[23] Schoukens J., Dobrowiecki, T. and Pintelon, R., "Parametric Identification of Linear Systems in the Presence of Nonlinear Distortions. A Frequency Domain Approach," *IEEE Trans. Autom. Contr.*, vol. AC-43, no. 2, pp. 176-190, 1998.

[24] Enqvist, M. and Ljung, L., "Linear approximations of nonlinear FIR systems for separable input processes," *Automatica*, vol. 41, no. 3, pp. 459–473, 2005.

[25] Schoukens, J., Lataire, J., Pintelon, R., Vandersteen, G., and Dobrowiecki, T., "Robustness issues of the equivalent linear representation of a nonlinear system," *IEEE Trans. Instrum. and Meas.*, vol. 58, no. 5, pp. 1737-1745, 2009.

[26] Pintelon, R., Louarroudi, E., and Lataire, J., "Detection and quantification of the influence of time variation in frequency response function measurements using arbitrary excitations," *IEEE Trans. Instrum. and Meas.*, vol. 61, no. 12, pp. 3387-3395, 2012.

[27] Pintelon, R., Schoukens, J., Vandersteen, G., and Barbé, K., "Estimation of nonparametric noise and FRF models for multivariable systems - Part I: theory. *Mechanical Systems and Signal Processing*," vol. 24, no. 3, pp. 573-595, 2010.

[28] Pintelon, R., Vandersteen, G. , Schoukens, J., and Rolain, Y., "Improved (non-)parametric identification of dynamic systems excited by periodic signals - The multivariate case," *Mechanical Systems and Signal Processing*, vol. 25, no. 8, pp. 2892-2922, 2011.

[29] Bowen, M. K., and Smith, R., "Derivative formulae and errors for non-uniformly spaced points," *Proceedings of the Royal Society A*, vol. 461, no. 2059, pp. 1975-1997, 2005.

[30] Pintelon, R., Louarroudi, E., and Lataire, J., "Simulation example of a weakly nonlinear, arbitrarily time-varying system excited by periodic inputs," *Internal Note*, dept. ELEC, Vrije Universiteit Brussel, 2015.

[31] Ralston, A., and Rabinowitz, P., *A First Course in Numerical Analysis*. New York (USA): McGraw-Hill, 1984.